SIDE-LOOKING RADAR IMAGERY APPLIED TO MAPPING

Dr. Franz Leberl
Institute for National Surveying and Photogrammetry
Technical University Graz
Austria

ABSTRACT

Some important applications of air- and spaceborne side-looking radar images to mapping problems are being reviewed. Basic facts about radargrammetric formulas are pointed out. Mapping applications discussed concern cartography, geology, oceanography, lake and sea ice.

1. INTRODUCTION

The development of applications of Side-Looking Radar (SLR) imagery to mapping tasks was in the past largely in the hands of military agencies. Recently, however, civilian radar mapping research had a major boost through the decision of the US National Aeronautics and Space Administration to launch radar into Earth orbits (SEASAT, Space Shuttle OFT-2, Spacelab). The basic formulations of radargrammetry and numerous radar mapping applications are thus being considered at many research institutes. A review paper (Leberl, 1976) gives an outline of the present status of SLR mapping for cartographic purposes. Some of the major points of ongoing developments will be described in the following in order to complement the above mentioned review.

2. BASIC RADARGRAMMETRIC FORMULATIONS

Brute force and synthetic aperture radar have been treated in the past without attention to their basic differences: the geometric problems of converting signal histories into map films in Synthetic Aperture Radar (SAR) has not received attention. However, in view of digital correlation of satellite SAR data this problem is presently moving into the focus of radargrammetric research workers.

Radargrammetric formulas have been reviewed by Leberl (1976) with an outline of the difference between real and synthetic aperture radar: in the first case the image geometry is defined by

the sensor position and attitude, in the second case it is defined by the velocity vector. Concepts such as squint were explained. This is important in satellite radar and radar stereo since squint can and will be used to compensate for perturbations due to relative motions between the satellite and the revolving Earth. Also, squint is often erroneously seen as a tool to achieve single flight stereo convergence of radar projection rays.

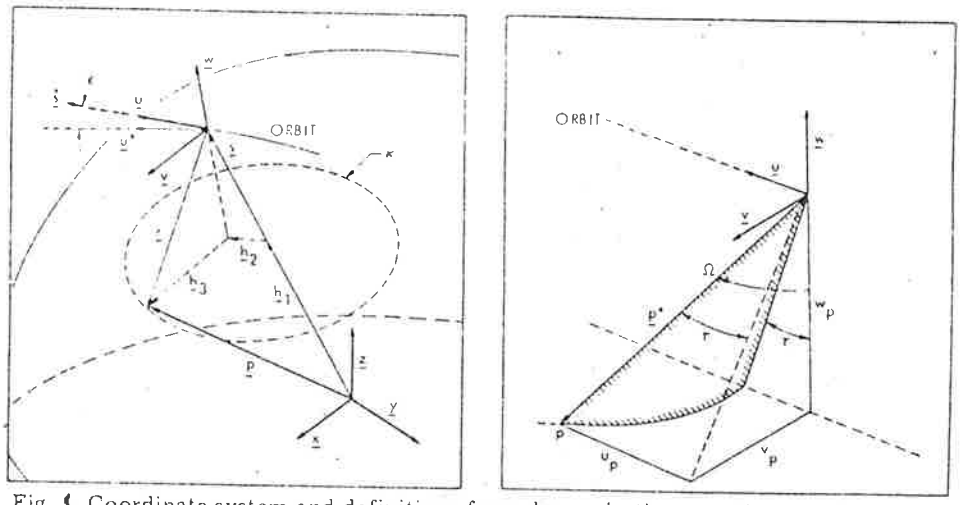

Fig. 1. Coordinate system and definitions for radar projection equations. a. Planetocentric and antenna systems, K = intersection of range sphere and planetary surface (reference figure). b. Cone complement angle, τ and vector p^* / from : Leberl, 1976).

According to Figure 1 we obtain the basic projection equation as:

$$\underline{p} = \underline{s} + \underline{r} \tag{1}$$

$$\underline{r} = u_p \underline{u} + v_p \underline{v} + w_p \underline{w} \tag{2}$$

$$u_p = r \sin \tau$$

$$v_p = r \left(\sin^2 \Omega - \sin^2 \tau\right)^{1/2} \tag{3}$$

$$w_p = r \left(-\cos \Omega\right)$$

or:

$$\underline{p} = \underline{s} + \underline{A}\, \underline{p}^* \tag{4}$$

$$\underline{A} = (\underline{u}, \underline{v}, \underline{w}) = \begin{bmatrix} u_1 & v_1 & w_1 \\ u_2 & v_2 & w_2 \\ u_3 & v_3 & w_3 \end{bmatrix} \tag{5}$$

With real aperture radar, matrix $\underline{A}$ is a rotation matrix defined by the classical photogrammetric rotation angles φ, ω, κ. With SAR, $\underline{A}$ is a function of the velocity vector $\dot{\underline{s}}$:

$$\underline{u} = \dot{\underline{s}} / |\dot{\underline{s}}|$$

$$\underline{v} = (\underline{s} \times \dot{\underline{s}}) \,/\, |\underline{s} \times \dot{\underline{s}}| \tag{6}$$

$$\underline{w} = (\underline{u} \times \underline{v}) \,/\, |\underline{u} \times \underline{v}|$$

Position vector $\underline{s}$ may be replaced by the local vertical if another than the planetocentric coordinate system is used.

Equs. (1), (2) and (3) can be transformed to:

$$\tan\gamma = \frac{u_p}{(v_p^2 + w_p^2)^{1/2}} = \frac{u_1\,(p_1-s_1) + v_1\,(p_2-s_2) + w_1\,(p_3-s_3)}{(\sum_{i=2}^{3}(u_i\,(p_1-s_1) + v_i\,(p_2-s_2) + w_i\,(p_3-s_3))^2)^{1/2}} \tag{7}$$

$$r = |\underline{r}| = (u_p^2 + v_p^2 + w_p^2)^{1/2} = |\underline{p} - \underline{s}| \tag{8}$$

Equation (7) represents a cone, Equ. (8) a sphere. The intersection is a cercle concentric with respect to the velocity vector defined by $\dot{\underline{s}}$ or the longitudinal axis of the antenna.

A number of algorithms for single image and stereo mapping have been developed on the basis of Equs. (1) to (8). Details may be found in Leberl (1976).

3. RADAR MAPPING APPLICATIONS

3.1 Basic Mapping of Terrestrial Land Features

Numerous projects of original mapping with airborne radar were carried out since about 1967, mainly but not only in tropical areas. The begin was made in Panama, presently a number of african nations are in the process of being mapped with radar. The standard mapping product consists of "semi-" controlled image mosaics. "Semi-" implies here the use of ground control, but no rectification of the original images. Methods of mosaicking were analysed in an experiment in the USA (Leberl, Jensen and Kaplan, 1976).

The potential of radar mapping has not been realized in these projects: rectification, stereo mapping, auxiliary information from other images etc. have not been advanced into the practical application. Only two-dimensional (planimetric) block adjustment has been used in at least two projects (Leberl, 1976), and research studies were completed by two authors on 3D-adjustment (DBA-Systems, 1974; Dowideit, 1977). Achieved

accuracies are presented in Table 1: with high density of control accuracies can be made quite high, of the order of magnitude of the radar ground resolution.

Author	Accuracy Plan. (m)	Height (m)	Number of Control Pts.	Number of Radar Strips	Control Density Pts. per 100 000km^2
Leberl et al.	± 150	---	16	24	17.7
-"-	± 400	---	4	24	4.4
DBA	± 20	± 15		3	1200
Dowideit	± 50	± 35	34	3	216

Table 1: Accuracies of Radar Block Adjustments

3.2 Basic Mapping of Non-Terrestrial (Planetary) Surfaces

Non-terrestrial mapping with radar was possible on the Moon using Apollo 17 satellite radar data as shown in Figure 2. The visual appearance of the orbital radar images is explained in Figure 3. The slant range presentation leads to the impression that the relief is rolled onto a cylinder.

The results that were obtained have been described previously (Leberl, 1977). Accuracies were limited by the particular imaging arrangement employed: single image mapping was accurate to within ± 200 m (coordinate errors) due to steep look angles and effects of the terrain relief, low resolution and poor error propagation.

Stereo mapping produced height errors of only + 150 m, in spite of very small stereo intersection angles of only about 2°. This is due to the steep look angles too, which, however, led to large errors of the cross-track coordinate of ± 500 m. The possibilities of radar stereo mapping from orbital radar could be demonstrated. A major improvement is only possible by increased stereo intersection angles, e.g. through changed look angles in adjacent orbits.

3.3 Geological Mapping

The fact that topographic features, lineaments, texture, vegetation lines, drainage patterns and fault scarps are shown leads to great potential of radar for geological mapping. Radar backscatter is related to surface roughness and dielectric constant

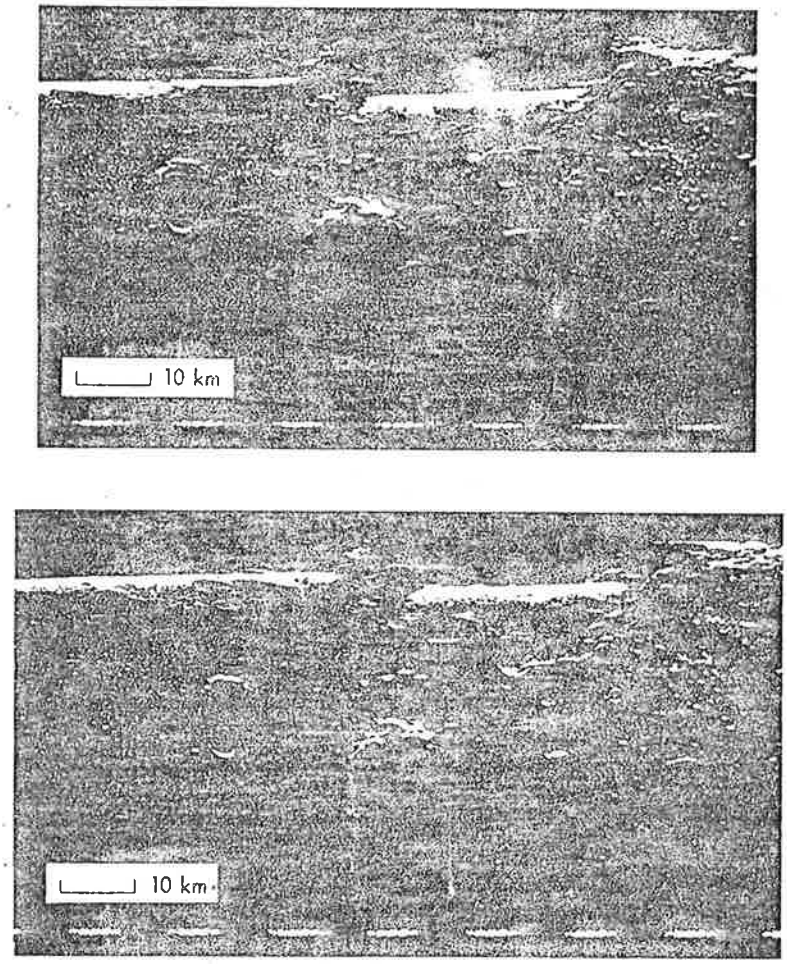

Fig. 2. ALSE-VHF side-looking orbital radar images of crater Maraldi on the Moon. Images were produced during revolutions 25 and 26 of the Apollo 17 command module

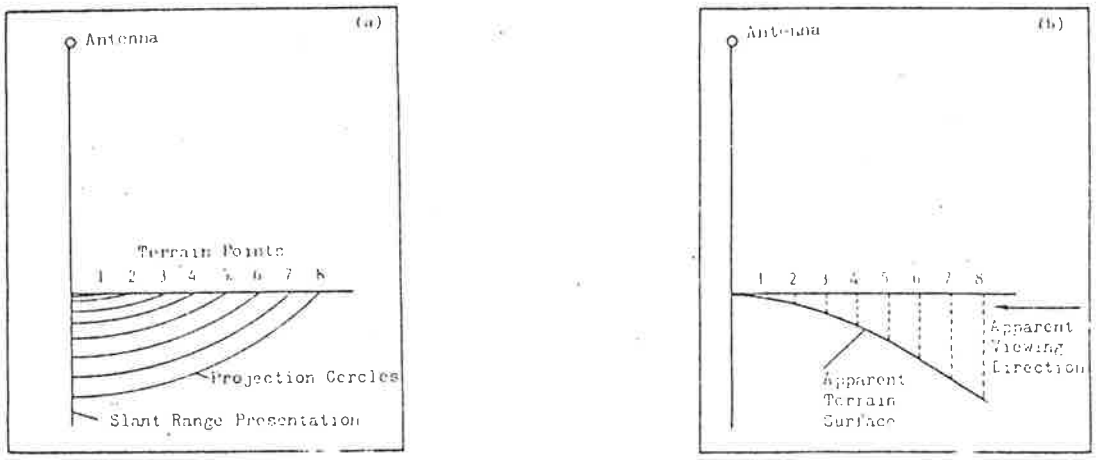

Figure 3: Explanation of the panoramic visual effect when viewing a radar slant range presentation.

Figure 4: Digitally processed synthetic aperture radar (L-band) is composed with LANDSAT image of Death Valley, California.

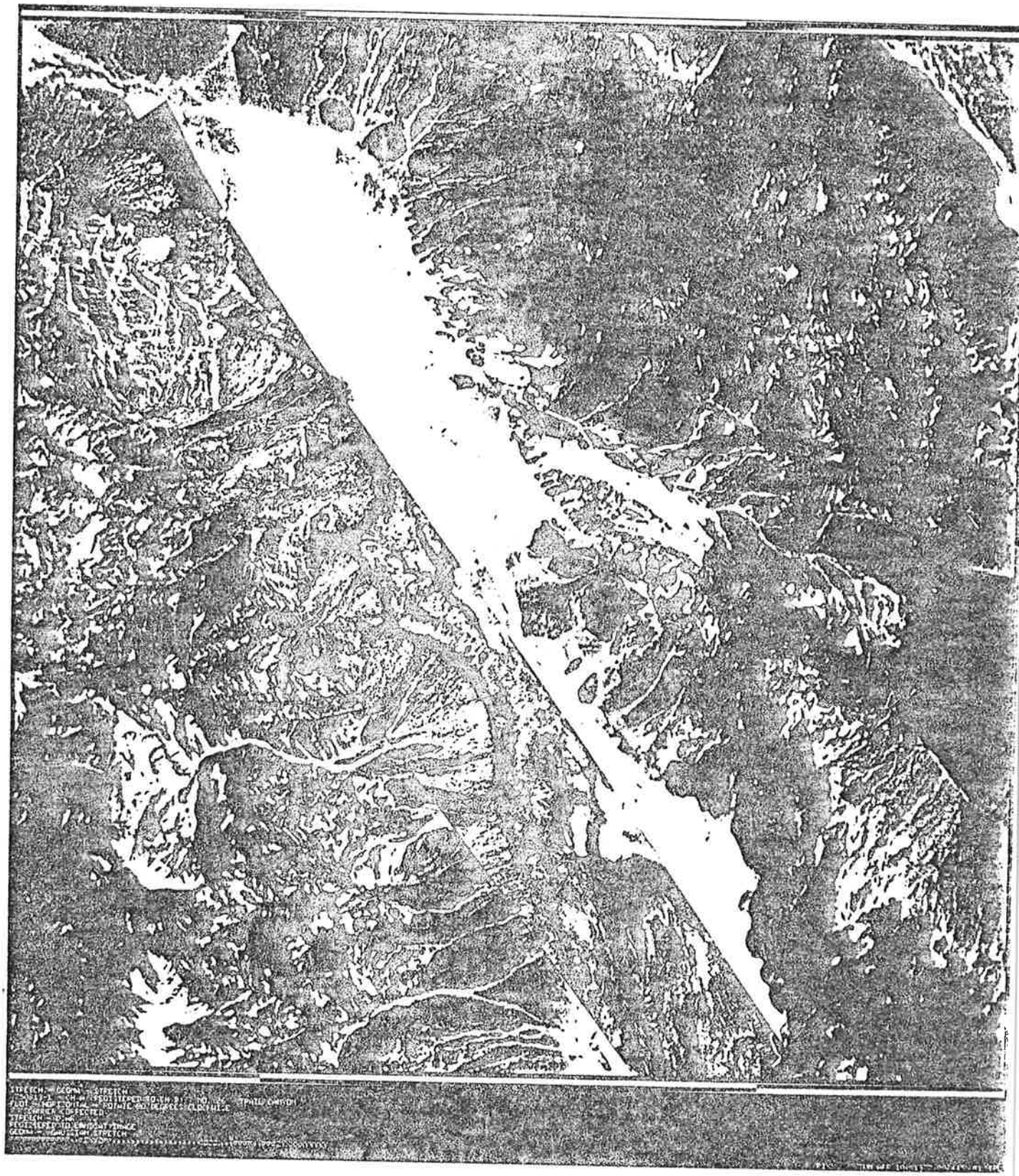

which permits classification of a region into different classes of backscattering units.

Research is just starting in the area of interpreting multi-spectral radar in conjunction with other image types. Figure 4 shows an example of a digitally processed composite of radar and Landsat. This is different from previous work (Harris and Graham, 1976) in that both components (Landsat and Radar) were treated digitally.

3.4 Oceanography

SEASAT will be the beginning of radar mapping of ocean surface features. Ocean waves have been imaged with airborne radar under a variety of conditions. Internal waves, current boundaries, weather fronts, eddies and ship wakes have been imaged. Evidently, radar can be of great value since these ocean surface features can be monitored in an all-weather / day and night environment.

3.5 Sea and Lake Ice

Radar mapping of lake and sea ice has been carried out in a number of different occasions. A recent demonstration was poosible in the Arctic Ice Dynamics Joint Experiment (AIDJEX). The frequent cloud cover and fog and poor visibility conditions in the arctic region make radar a significant tool for surveillance and mapping.

Figures 5 and 6 illustrate the measurement of sea ice drift from images taken at different times. Absolute accuracy (without ground control) is about $\pm$ 2km. Relative accuracy (within one image or mosaic) is about $\pm$0.1 km to $\pm$0.2 km, limited by resolution, look angles, accuracy of feature definition and stability of navigation.

3.6 Other Applications

There are numerous other potemtial applications of radar imagery at different levels of maturity. High importance is attached to the measurement of snow and soil moisture content, identification of vegetation types and assessment of its health. Investigations also concern land-use and urban mapping. In many instances this is only at an initial stage of investigation.

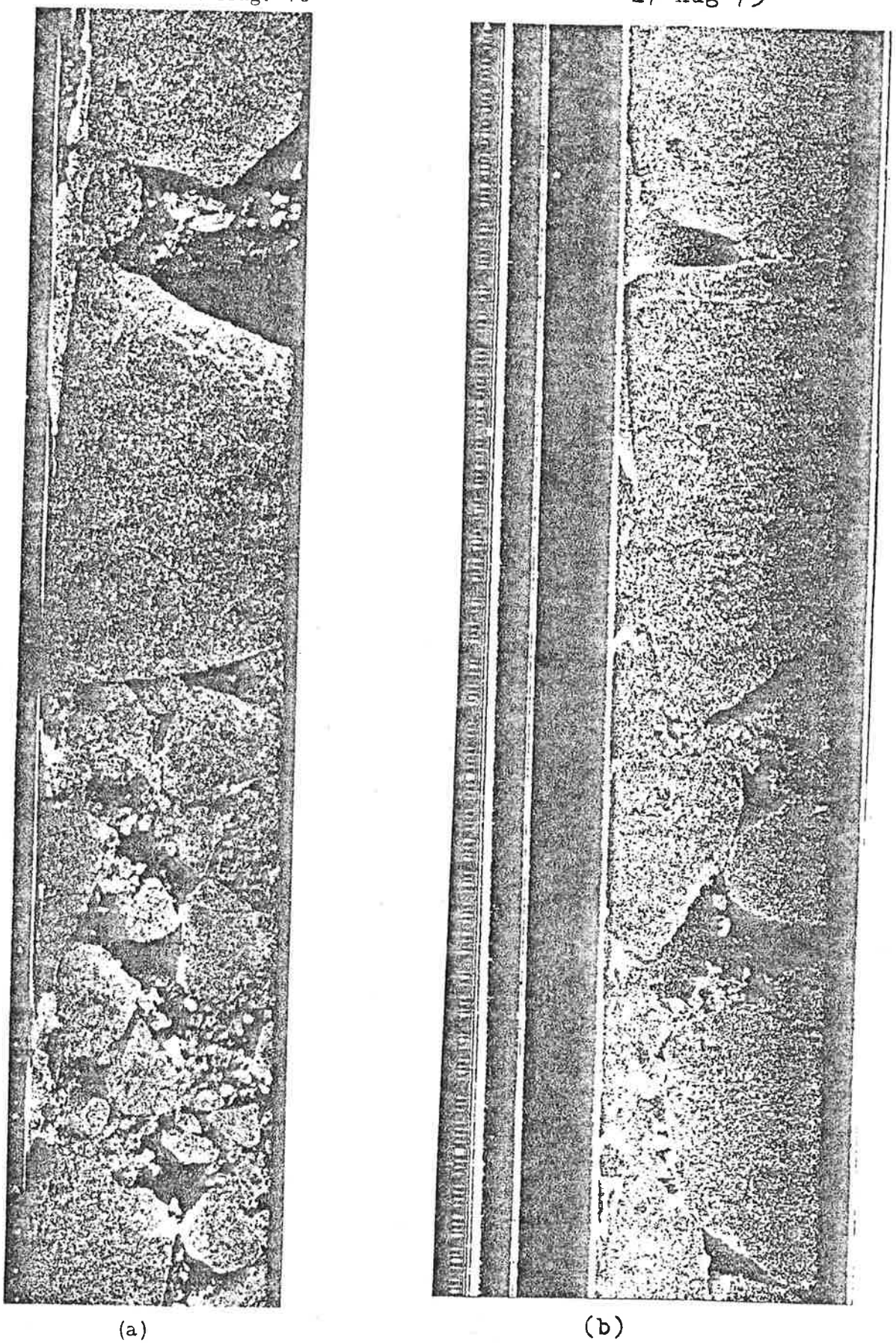

Figure 5: Pair of airborne synthetic aperture radar images at L-band, taken in the arctic ocean

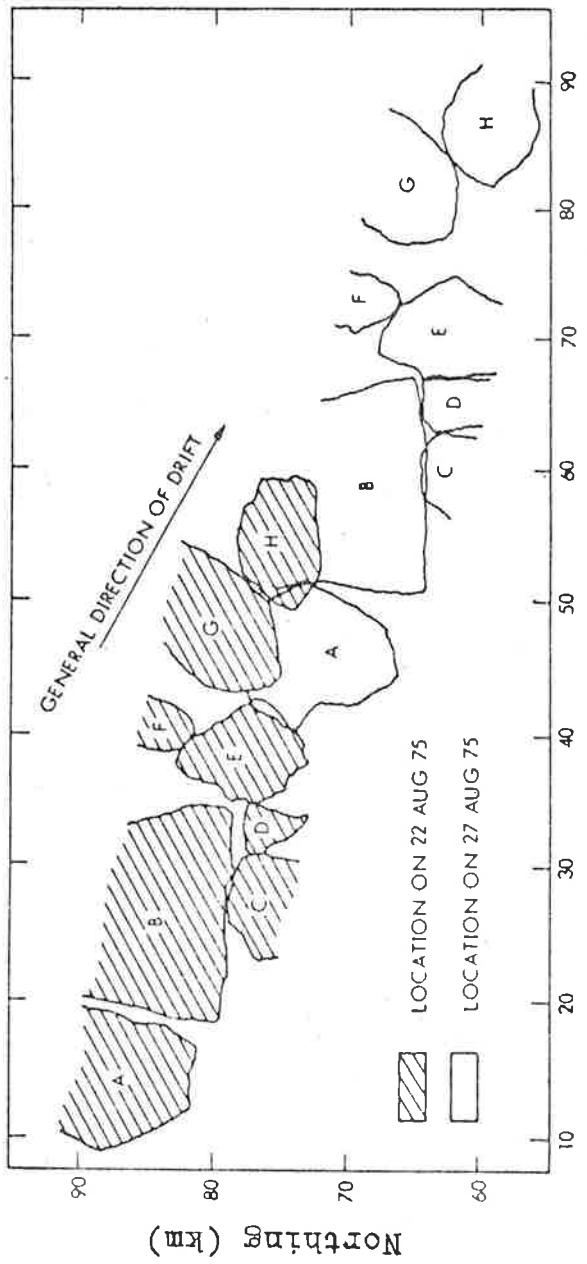

Figure 6: Map of arctic sea ice drift, measured from the radar images shown in Figure 5.

4. CONCLUSION

Research on Earth science application of radar images seems to have just been intensified after a period of relative stagnation when efforts were concentrated on satellite scanning (LANDSAT). The main thrust is in oceanographic and sea ice applications.

The main advantages of radar imaging are its penetration capability (e.g. clouds) and its active mode of operation (day and night). Other characteristics (polarisation, choice of look angle etc.) may contribute to its value too. These advantages may well lead to expect continued and increasing importance of radar in Earth science applications.

REFERENCES

DBA-Systems (1974) "Research Studies and Investigations for Radar Control Extensions", DBA-Systems Inc., Melbourne, Florida.

Dowideit G. (1977) "Eine Blockausgleichung für Abbildungen des seitwärts schauenden RADAR (SLAR)", Wiss. Arb., Lehrstühle für Geodäsie, Photogrammetrie und Kartographie, Nr. 75, T.U. Hannover, F.R.G.

Harris G., L.C. Graham (1976) "Radar-Landsat Synergism", Pres. Paper, 13th Congress of ISP, Helsinki, Finland.

Leberl F. (1976) "Imaging Radar Applications to Mapping and Charting", Photogrammetria, Vol. 32

Leberl F., H. Jensen, J. Kaplan (1976) "Side-Looking Radar Mosaicking Experiment" Photogrammetric Engineering and Remote Sensing, Vol. 42, No. 8

Leberl F. (1977) "Mapping the Lunar Surface from Side-Looking Radar Imagery", The Moon, Vol. 15.